Resonant, Elliptical-Polarization Control of Microwave Ionization of Hydrogen Atoms

M. R. W. Bellermann,[1] P. M. Koch,[1] and D. Richards[2]
[1]*Department of Physics, State University of New York, Stony Brook, New York 11794-3800*
[2]*Mathematics Faculty, Open University, Milton Keynes, MK7 6AA, United Kingdom*
(Received 8 January 1997)

For certain ranges of the principal quantum number $n_0 \gg 1$ a few units wide, ionization of hydrogen atoms by a 9.904 GHz electric field is observed to be extremely sensitive to elliptical polarization. Classical 3D Monte Carlo calculations quantitatively reproduce the experimental data. Classical theory shows that the observed sensitivity to elliptical polarization is a resonant effect in this strongly driven quantal system. The resonant dynamics provides a mechanism for controlling the ionization. [S0031-9007(97)03198-0]

PACS numbers: 32.80.Rm, 05.45.+b, 42.50.Hz

The sensitivity of atoms and molecules to electromagnetic fields can be used to manipulate their behavior. Some examples demonstrate the variety of schemes being investigated for control of quantum systems. An historically important and simple one for two-level systems uses resonant π or $\frac{\pi}{2}$ pulse(s) [1]; this was later generalized to multilevel systems [2]. More subtle control schemes vary frequencies, relative phases, and field polarization.

Variation of the relative phase of a laser field and its (second or third) harmonic was used to control atomic ionization [3], molecular photodissociation [4], and high-harmonic production [5]. Two non-phase-coherent laser fields were used to control electromagnetically induced transparency [6], atomic ionization [7], and molecular photodissociation [8]. Control of the field polarization was investigated for producing subfemtosecond laser pulses [9], high harmonics [10], and hot above-threshold-ionization electrons [11], used in [12] to pump a vacuum-ultraviolet laser transition.

This Letter demonstrates experimentally and theoretically how field parameters can be set to control the ionization rate of excited H atoms. Unlike all previous examples of control of a driven quantal system, classical theory quantitatively reproduces our experimental data. This gives great insight into the physics.

Our experiment used established techniques [13] for preparing, via two-step laser excitation, a 14.6 keV beam of H atoms in a uniform distribution of substates with a given n_0 in the range 31–45. The beam traversed the $\omega/2\pi = 9.904$ GHz field inside a cavity [14]. For the given range of n_0, the scaled frequency [13,15], which is the ratio of ω and the initial classical Kepler frequency ω_K, is $0.0449 \leq n_0^3\omega \equiv \Omega_0 \leq 0.137$. Because Ref. [16] describes the measurement and control of the amplitude and polarization of the cavity field, only a few details are given here. (Hereafter LP, CP, and EP will mean linear, circular, and elliptical polarization, respectively.) Microwaves fed through two arms and injected through two off-axis slits in the entrance end cap created [14] the on-axis field $\mathbf{F}(t) = \lambda(t)\mathcal{F}[\hat{\mathbf{X}}\alpha\sin(\omega t) + \hat{\mathbf{Y}}\sin(\omega t + \delta)]$, with $0 \leq \alpha \leq 1$ and $0 \leq \delta \leq \frac{\pi}{2}$; $\lambda(t)$ is the half-sine, 152 cycle, pulse envelope experienced by the atoms traversing the cavity, and (X, Y, Z) are spatial coordinates in the laboratory frame. The ratio $F/\mathcal{F}$ of the peak amplitude F to the amplitude $\mathcal{F}$ of the $\hat{\mathbf{Y}}$ component depends on the polarization. With an attenuator in one arm, to control α, and a phase shifter in the other, to control δ, we used the atoms to fine-tune the polarization to CP [16,17], giving $\alpha = 1.00 \pm 0.05$ and $\delta = 90° \pm 1°$. Extinguishing the power in one arm ($\alpha \leq 0.0002$) created LP. To create EP one could either (i) keep $\alpha = 1$ and vary δ or (ii) make $\alpha < 1$ and keep $\delta = \pi/2$ or (iii) vary both α and δ. Experimentally it was more precise to use scheme (ii), but for comparisons with theory to be made below, it will be easier to characterize the EP via scheme (i), for which $F/\mathcal{F} = \sqrt{2}\cos(\delta/2)$ varies from 1, at CP, to $\sqrt{2}$, at LP.

Ionization in a downstream, 9.8 GHz cavity was used to detect highly excited atoms. The loss of such atoms by ionization in the 9.904 GHz cavity was the experimental signal recorded [18].

Before demonstrating and understanding the use of EP for resonant control of the ionization dynamics, we need to recall well-known features of ionization of excited H atoms by a static, an LP, and a CP field. Hereafter using atomic units (au) unless explicitly noted, the Hamiltonian is $\mathcal{H}(t) = p^2/2 - 1/R + \mathbf{R}\cdot\mathbf{F}(t)$. For a static field, $\mathbf{R}\cdot\mathbf{F}(t) = ZF$, the system is separable in parabolic coordinates (ξ, η, ϕ) [19]. Below the onset of ionization, all three classical actions $\mathbf{I} \equiv (I_\xi, I_\eta, I_m)$ [quantum numbers (n_1, n_2, m)] are conserved. Classically, there is a sharp threshold field $F_{\rm crit}(\mathbf{I})$ below which the motion with these actions remains bound; from the least robust orbit [quantally, $m = n_1 = 0, n_2 = (n-1)$] to the most robust orbit [$n_1 = (n-1)$, $n_2 = m = 0$], $n_0^4 F_{\rm crit}$ varies between about 0.13–0.38. Tunneling through the η barrier allows ionization for $F < F_{\rm crit}$; for interaction times near 10^{-8} s and $n_0 \simeq 40$, it lowers thresholds by 10%–15% [13,20].

For an LP field, $\mathbf{R}\cdot\mathbf{F}(t) = \lambda(t)ZF\sin(\omega t + \psi)$, with ψ an initial phase; again, separability leads to conservation of $|m|$. The dynamics is quasistatic [13,21] if Ω_0 is sufficiently small and away from exponentially sharp resonances discussed theoretically for 1D in [22]. The

 0031-9007/97/78(20)/3840(4)$10.00

spatial reversal of F on each half-cycle interchanges n_1 and n_2; therefore, as Fig. 1 of [21] shows, for a uniform mixture of substates of a given n_0, classically a microcanonical ensemble, the ionization probability $P_{\rm ion}$ rises from 0 to 1 as the scaled amplitude $n_0^4 F \equiv F_0$, which is the ratio of the peak electric field amplitude to the Coulomb field at the Bohr orbit for the initial n_0 value [13,15], varies between about 0.115–0.17. This is just the beginning of the wider classical range, $F_0 = 0.13$–0.38, lowered 10%–15% by tunneling, discussed above for the static field case.

In a frame (x, y, z) rotating at frequency ω about the proton, $\mathcal{H}(t)$ becomes $K(t) = p^2/2 - 1/r + \lambda(t)\mathcal{F}y + \omega L_z + 0.5\lambda(t)\mathcal{F}[\,y \sin 2\omega t - x(1 - \cos 2\omega t)]\sin\delta_1 + 0.5\lambda(t)\mathcal{F}[x \sin 2\omega t - y(1 + \cos 2\omega t)]\sin^2(\delta_1/2)$, where $\delta_1 = \pi/2 - \delta$. Notice that $0 < \delta_1 < \pi/2$ gives EP, and driving terms at 2ω appear in the dynamics in the rotating frame [17,23,24]. We confirmed that the rotational term ωL_z has little effect on $P_{\rm ion}$ for $\Omega_0 \lesssim 0.1$ by finding close similarity between classical trajectory ionization curves calculated with (the CP case) and without (the static field case) the ωL_z term. Therefore, at low Ω_0 the lack of interchange of n_1 and n_2 (see above) should cause quantal CP ionization curves to "stretch out" and approach $P_{\rm ion} = 1$ at a higher value of F_0 than for the LP case.

The inset to Fig. 1 shows experimental ionization curves for $n_0 = 45$, one of many cases with relatively little polarization dependence. For $P_{\rm ion} \lesssim 0.2$, varying the polarization has little effect. That the CP curve approaches $P_{\rm ion} = 1$ only when F_0 is much larger than for the other curves, however, is the anticipated stretching out.

The main part of Fig. 1 shows ionization curves for $n_0 = 42$, only 3 n_0 units lower. Qualitatively, the polarization dependence is similar to that for $n_0 = 45$, but with one exception: the $n_0 = 42$ curve for $\delta = 0.45\pi$ ($\delta_1 = 0.05\pi$) initially rises with the LP and other EP curves but then passes through a local maximum near $P_{\rm ion} = 0.85$, followed by a gentle local minimum; its final, slow rise toward $P_{\rm ion} = 1$ is similar to the CP curve.

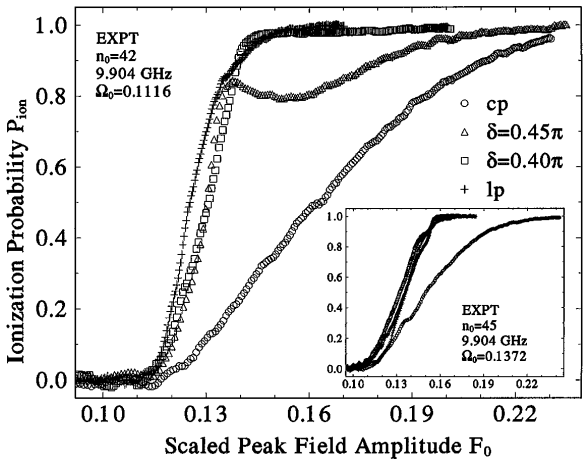

FIG. 1. A survey of the polarization dependence for experimental ionization curves for $n_0 = 42$ and $n_0 = 45$ (inset).

Figure 2 shows the EP dependence for $n_0 = 42$ from $\delta = 0.42\pi$ to 0.5π, with an uncertainty $\Delta\delta = 0.01\pi$. The remarkable local variation of $P_{\rm ion}$ with δ at fixed F_0 allows for significant control of ionization. Sensitivity is greatest near $F_0 = 0.14$, where decreasing δ from 0.5π (CP) to 0.42π increases $P_{\rm ion}$ about fourfold. Over about the same range of δ, we observed (data not shown here) similar EP dependence for $n_0 = 41$ and 43, but *not* for $n_0 \gtrsim 44$ nor, with exceptions discussed below, for $n_0 \lesssim 40$.

We now discuss classically the physical origin of the sensitivity of $n_0 = 41, 42, 43$ at 9.904 GHz to EP for values of δ close to CP; mathematical details of the theory are given in [24]. A full understanding of the polarization-dependent dynamics will require 3D quantal calculations, but state-of-the-art 3D quantal (Floquet) calculations have been reported, so far, only for LP and CP and for $n_0 \lesssim 23$ [25]. Until improvements in computers and algorithms enable 3D quantal calculations for 3D H atoms in an EP field, with the atomic and field parameters used for this Letter, we must use insights gleaned from comparisons of experimental data with classical calculations and theory.

We begin with 3D classical Monte Carlo calculations (3dCL) [16,21,26] that closely modeled the experiment, including $\lambda(t)$ and the initial substate distribution. Each computation used a stratified sample [27] of N orbits ($= 3^5$, except where specifically noted) chosen from a microcanonical ensemble [15]. If j orbits ionized, $P_{\rm ion} = j/N$, and with greater than 67% probability the actual classical $P_{\rm ion}$ lies within the range $P_{\rm ion} \pm [P_{\rm ion}(1 - P_{\rm ion})/N]^{1/2}$; e.g., for $P_{\rm ion} = \{0.1\}, 0.5, [0.9]$ and $N = 3^5$, the formula gives the relative error $\{\pm 1.9\%\}, \pm 3.2\%, [\pm 1.9\%]$.

Allowing for the $\pm 0.01\pi$ experimental uncertainty in δ, the remarkable, quantitative agreement between the experimental data and 3dCL results in Fig. 2 for $n_0 = 42$ (also for $n_0 = 41$ and 43, not shown here) validates the

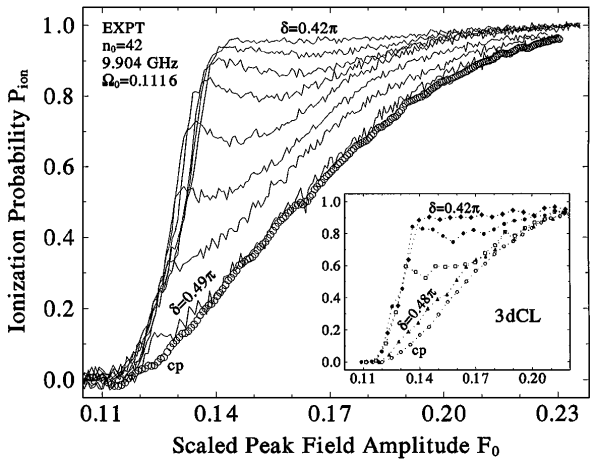

FIG. 2. Detailed elliptical-polarization dependence for $n_0 = 42$ in steps of $\delta/\pi = 0.01$ [$\delta/\pi = 0.02$] for experimental data [for 3dCL calculations (inset)].

use of classical theory to understand the extreme local sensitivity of the ionization dynamics to polarization.

Two questions arise from these data: (i) What produces the local maximum in $P_{\rm ion}$ at, e.g., $F_0 \simeq 0.13$ for $\delta \simeq 0.45\pi$? (ii) Why does it have this effect?

Answering (i) is relatively simple. Answering (ii) is more difficult because it involves understanding the complex details of multidimensional dynamics. The key point is that all perturbations vary little during an unperturbed Kepler period, so one can average over this fast motion, reducing the number of degrees of freedom, and then write the resulting equations for the mean motion in terms of the vectors $\mathbf{X} = \mathbf{L} - \mathbf{A}$ and $\mathbf{Y} = \mathbf{L} + \mathbf{A}$ where $\mathbf{L}$ is the orbital angular momentum and $\mathbf{A} = (\mathbf{p} \times \mathbf{L} - \mathbf{r}/r)/\sqrt{-2E}$ is the Runge-Lenz vector. For a CP field ($\delta_1 = 0$), both $\mathbf{X}$ and $\mathbf{Y}$ rotate uniformly about the field direction with the scaled frequency $\overline{\omega} = \sqrt{\omega_S^2 + \Omega_0^2}$, where $\omega_S = 3\mathcal{F}_0/2$ is the classical Stark frequency associated with the scaled amplitude $\mathcal{F}_0$. For the ranges of F_0 and Ω_0 in this Letter, $\overline{\omega} < \frac{1}{3}$. Perturbations of frequency $2\Omega_0$ and strength proportional to δ_1, which appear for an EP field, can resonate with the mean motion when $\overline{\omega} = 2\Omega_0$, i.e., when $\mathcal{F}_0 \simeq \mathcal{F}_{0_r} \equiv 2\Omega_0/\sqrt{3}$. For $\Omega_0 = 0.1116$ this gives $\mathcal{F}_{0_r} = 0.13$; equivalently, this is F_{0_r} varying from 0.145 to 0.13 as δ/π varies from 0.42 to 0.5, in agreement with the local maxima in Fig. 2. We use "$2\Omega_0$ resonance" to label this dynamics.

The averaged equations of motion give a model for understanding how the resonance affects the bound-state dynamics. With the full richness of the details being given in [24], ionization is added *post hoc* to the model via the time dependence of $\mathcal{F}_{\rm crit}(t) = \mathcal{F}_{\rm crit}(\mathbf{I}(t))$, which can be used to mimic the classical escape over the barrier when $\mathcal{F}_{\rm crit}(t) < \lambda(t)\mathcal{F}$. [Recall that $0 \le \lambda(t) \le 1$ is the pulse envelope.] This model, compared with exact calculations in [24], shifts one's attention to understanding the temporal evolution of the classical actions $\mathbf{I}(t)$ and critical fields $\mathcal{F}_{\rm crit}(\mathbf{I}(t))$. Though the details are complicated, the analysis shows that if $I_m > 0$ [< 0] then $\mathcal{F}_{\rm crit}(t)$ decreases [increases] as $\lambda(t)\mathcal{F}$ increases through the resonance by an amount which increases as $d\lambda/dt$ decreases. Numerical calculations show that the mean over $I_m > 0$ and $I_m < 0$ is dominated by the behavior of the former, thereby producing the observed local maximum in the ionization probability [18].

For $n_0 = 31, 32, 33$ we also found extreme sensitivity to EP, but for lower values of δ than for the $2\Omega_0$ resonance. Figure 3 shows $n_0 = 31$ ionization curves obtained in successive runs for eight values of δ between 0.28π–0.45π ($F/\mathcal{F}$ between 1.28–1.08). Observe the clear similarity between Figs. 3 and 2. The inset shows that the 3dCL results, obtained for the same eight values of δ, again reproduce the experimental polarization dependence.

Though $K(t)$ has harmonic terms only at $2\Omega_0$, let us, nevertheless, extrapolate the frequency-matching condition to a "$4\Omega_0$ resonance": $4\Omega_0 = \bar{\omega} = \sqrt{(3\mathcal{F}_0/2)^2 + \Omega_0^2}$, giving $\Omega_0 = 0.39\mathcal{F}_0$. The classical static field ionization threshold, $\mathcal{F}_0 = 0.13$, gives $\Omega_0 = 0.05$; at 9.904 GHz this gives $n_0 = 32$, the middle of the three n_0 values where we observed extreme sensitivity to EP. This result cannot be accidental. It predicts that successive application in the rotating frame of perturbation theory, classical or quantal, will lead to resonances at even powers of Ω_0. The detailed derivation has been accomplished, so far, only classically and only for the $2\Omega_0$ resonance [24].

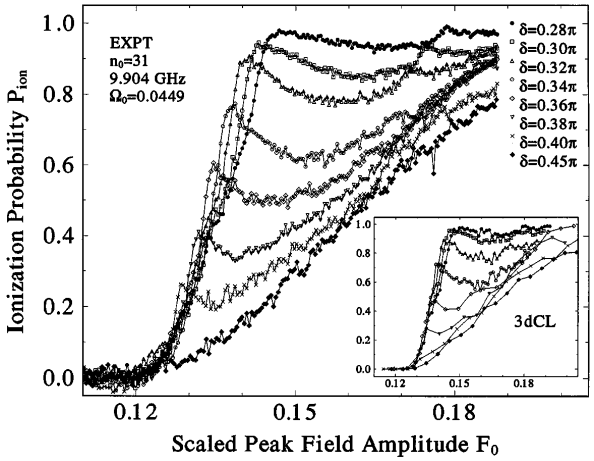

FIG. 3. Detailed elliptical-polarization dependence for $n_0 = 31$ for experimental data and for 3dCL calculations (inset).

Continuing further, postulate a "$6\Omega_0$ resonance": $6\Omega_0 = \bar{\omega} = \sqrt{(3\mathcal{F}_0/2)^2 + \Omega_0^2}$. The same conditions as above give $\Omega_0 = 0.25\mathcal{F}_0$ or $\Omega_0 = 0.033$ at $\mathcal{F}_0 = 0.13$; at 9.904 GHz this requires n_0 between 26 ($\Omega_0 = 0.027$) and 27 ($\Omega_0 = 0.030$). (3dCL results at $\Omega_0 \simeq 0.03$, not shown here, clearly show the resonance at $\mathcal{F}_0 \simeq 0.12$, $\delta \simeq 0.3\pi$.) Though our microwave amplifier had insufficient power to ionize H atoms with $n_0 < 29$, our data give tentative evidence for a $6\Omega_0$ resonance at $n_0 = 31$, for which $\Omega_0 = 0.0449$. At this higher Ω_0, the postulated frequency matching requires $\mathcal{F}_0 \simeq 0.18$. Because this significantly exceeds the ionization threshold, $\mathcal{F}_0 = 0.13$, the postulated resonance should occur well up on the $n_0 = 31$ ionization curves. Notice that between $F_0 = 0.16$–0.18, the top three experimental ionization curves in Fig. 3 indeed show a local rise. At 0.01π increments in δ between 0.30π–0.34π, Fig. 4 compares 3dCL results with experimental curves, each of which is the average of two runs. At the low value of $\Omega_0 = 0.045$ ($n_0 = 31$), the 3dCL calculations were very time consuming, but as a special test case for good statistics we ran a total of $N = 1728$ orbits for the $\delta = 0.31\pi$ case, giving a 2σ statistical uncertainty of $\le \pm 0.7\%$ at $P_{\rm ion} = 0.9$. Classical dynamics reproduces the clear, steplike, local rise in $P_{\rm ion}$ for the lower values of δ in Fig. 4 *and* its disappearance at larger values.

Note the following about the EP-induced resonances. Because the plateaulike feature in the top three curves in Fig. 3 (e.g., between about $F_0 = 0.145$–0.175 in the 0.28π curve) is near $P_{\rm ion} = 1$, most atoms in the

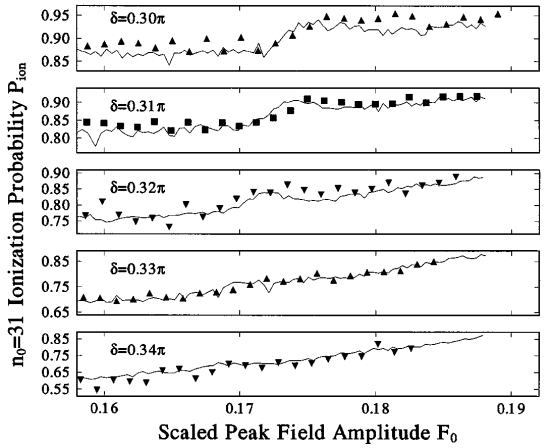

FIG. 4. Detailed elliptical-polarization dependence for $n_0 = 31$ for experimental data (solid curves) and for 3dCL calculations (inverted filled triangle: 432 orbits; upright filled triangle: 864 orbits; filled square: 1728 orbits).

ensemble have already ionized as the plateau is reached. Those that have *not* done so continue to resist ionization over a significant range of increasing F_0, but eventually they succumb to the (resonant) process. In the EP field, therefore, these curves exhibit two thresholds [28].

In summary, we have demonstrated how the polarization of the driving field can be used to control the microwave ionization of excited hydrogen atoms. Unlike most of the many control schemes being discussed in the literature, the present case can be understood classically: it does not rely on interference of quantal amplitudes, but only upon resonance effects. More theoretical work is required to understand *why* the EP-dependent resonant dynamics is so well reproduced classically. One comment is that the classical mean motion is well approximated by a linear Hamiltonian; therefore, the corresponding quantal evolution will be obtained *exactly* from classical paths [29]. Another comment is that classical motion for EP driving lacks integrals of the motion. The corresponding lack of conserved quantum numbers will lead to a large number of participating quantal states, a necessary, but not sufficient, condition for quantal/classical correspondence. We hope that understanding the details of this dynamics will help one to control other strongly driven quantal systems.

The NSF, EPSRC, and, early on, Schlumberger-Doll Research gave financial support. The late D. Mariani greatly helped the experiments get underway. S. Zelazny used H vs He atom data and He CP Floquet calculations to check the microwave field calibration.

[1] L. Allen and J. Eberly, *Optical Resonance and Two-Level Atoms* (Dover, Mineola, NY, 1987).
[2] M. Holthaus and B. Just, Phys. Rev. A **49**, 1950 (1994).
[3] See Y.-Y. Yin *et al.,* Phys. Rev. Lett. **69**, 2353 (1992); D. Schumacher and P. Bucksbaum, Phys. Rev. A **54**, 4271 (1996), and references therein.
[4] B. Sheehy, B. Walker, and L. DiMauro, Phys. Rev. Lett. **74**, 4799 (1995).
[5] S. Watanabe *et al.,* Phys. Rev. Lett. **73**, 2692 (1994).
[6] M. Xiao *et al.,* Phys. Rev. Lett. **74**, 666 (1995).
[7] F. Wang, C. Chen, and D. Elliott, Phys. Rev. Lett. **77**, 2416 (1996).
[8] A. Shnitman *et al.,* Phys. Rev. Lett. **76**, 2886 (1996).
[9] M. Ivanov *et al.,* Phys. Rev. Lett. **74**, 2933 (1995).
[10] P. Antoine *et al.,* Phys. Rev. A **53**, 1725 (1996).
[11] P. Corkum, N. Burnett, and F. Brunel, Phys. Rev. Lett. **62**, 1259 (1989).
[12] B. Lemoff *et al.,* Phys. Rev. Lett. **74**, 1574 (1995).
[13] P. Koch and K. van Leeuwen, Phys. Rep. **255**, 289 (1995).
[14] The 2.57 cm long, 6.350 cm diameter brass cavity had 0.41 cm diameter end cap holes on its axis, along which the 0.21 cm diameter beam passed. The unloaded quality factors of the two spatially orthogonal, frequency-degenerate TE_{121} modes were about 1.5×10^4. Adapting the calibration method described in B. Sauer *et al.,* Rev. Sci. Instrum. **62**, 189 (1991), we determined the absolute amplitude of the microwave field to 5%.
[15] J. Leopold and I. Percival, J. Phys. B **12**, 709 (1979), used a theoretical ionization criterion based on the compensated energy, which we found not to be useful for the low values of Ω_0 in this Letter. Our classical trajectory calculations took ionization as orbital excursions to radii much larger than (typically 10 times) the original value. The results were insensitive to this particular choice.
[16] M. Bellermann *et al.,* Phys. Rev. Lett. **76**, 892 (1996).
[17] P. Fu *et al.,* Phys. Rev. Lett. **64**, 511 (1990).
[18] The n-cutoff, see Sec. 2.3.3 of Ref. [13], was $n_c^q \simeq 110$. We believe that for the values of $n_0 \ll n_c^q$ and $\Omega_0 \ll 1$ considered in this Letter, true ionization was the dominant effect at 9.904 GHz for the following reason. Classical numerical calculations for LP fields [21,26] and those presented here for various polarizations show that at low Ω_0 most orbits either ionize or have a final principle action near the initial one: Classical ionization occurs via escape over a slowly changing barrier, and the vast majority of nonionizing orbits adiabatically adjust.
[19] D. Banks and J. Leopold, J. Phys. B **11**, 2833 (1978).
[20] P. Koch and D. Mariani, Phys. Rev. Lett. **46**, 1275 (1981).
[21] B. Sauer *et al.,* Phys. Rev. Lett. **68**, 468 (1992).
[22] P. Dando and D. Richards, J. Phys. B **26**, 3001 (1993).
[23] T. Gallagher, Mod. Phys. Lett. B **5**, 259 (1991).
[24] D. Richards (to be published).
[25] LP: A. Buchleitner and D. Delande, Phys. Rev. Lett. **75**, 1487 (1995); CP: D. Delande, J. Zakrzewski, and A. Buchleitner, Europhys. Lett. **32**, 107 (1995).
[26] D. Richards *et al.,* J. Phys. B **22**, 1307 (1989); O. Rath, Ph.D. thesis, The Open University, 1990 (unpublished); O. Rath and D. Richards (to be published).
[27] J. Hammersley and D. Handscomb, *Monte Carlo Methods* (Methuen, London, 1964).
[28] In Fig. 3 tunneling causes the experimental curves to rise at $F_0 \simeq 0.12$, before the corresponding 3dCL rise at $F_0 \simeq 0.13$; see M. Bellermann, P. Koch, and D. Richards, Bull. Am. Phys. Soc. **41**, 1092 (1996).
[29] R. Feynman and A. Hibbs, *Quantum Mechanics and Path Integrals* (McGraw-Hill, New York, 1965).